

An analytical Machining models based on Flow Stress Properties for Non-Heat Treated and Heat Treated AISI 4140 Steel

Tae Hong Lee*

(논문접수일 2010. 08. 24, 수정일 2011. 03. 18, 심사완료일 2011. 05. 03)

열처리 및 비 열처리 AISI4140강의 유동응력 물성치를
기초로 하는 해석적 가공 모델 연구

이태홍*

Abstract

In this study, an experimental and theoretical program were carried out to determine the cutting forces and chip formation at different cutting speeds using a 0.4mm nose radius ceramic insert and -7° rake angle for non heat-treated AISI 4140 (27HRc) and heat-treated AISI 4140 (45 HRc) steel. The results obtained were compared to show the hardness differences between the materials. The secondary deformation zone thicknesses when comparing the two materials show different physical structure but similar size. These results were also discussed in light of the heat treatment and the effects it had on the machining characteristics of the material. In addition, the Oxley Machining Theory was used to predict the cutting forces for these materials and a comparison made. The predicted cutting performances were verified experimentally and showed good agreement with experimental data.

Key Words : Oxley machining Theory(Oxley 이론), Material properties(재료 물성치), Cutting forces(절삭력), Chip Formation(칩 형상)

NOMENCLATURE

| | | | |
|-----------------|--|-----------|---|
| C_s | Side cutting edge angle | h_1 | interface |
| d | Depth of cut (mm) | h_2 | Uncut chip thickness (mm) |
| f | Feed rate (mm/rev) | n | Chip thickness (mm) |
| F_c | Cutting force (N) | T | Strain hardening index |
| F_T | Thrust force (N) | T_{mod} | Temperature ($^\circ\text{C}$) |
| F_x, F_y, F_z | Three force components (N) | U | Velocity Modified Temperature ($^\circ\text{C}$) |
| k_{chip} | Shear flow stress in chip at tool-chip | δ | Cutting speed in m/min |
| | | | Ratio of tool chip interface plastic zone thickness to chip thickness |

* Research Center, Hyundai WIA (leeth@hyundai-wia.com)
Advanced Research Team, 8F, #462-18 Samdong, Uiwang, Kyunggi

| | |
|---------------------|---|
| ε | Uniaxial strain |
| $\dot{\varepsilon}$ | Uniaxial strain-rate |
| σ | Uniaxial flow stress |
| σ_1 | Value of σ at strain $\varepsilon=1$ |
| ϕ | Shear angle |
| γ | Rake angle |
| δh_2 | Secondary deformation zone thickness (mm) |
| τ_{int} | Shear stress in tool-chip interface |

1. Introduction

In attempting to predict machining performance analytical models based on material properties can be used. In using the analytical models, the flow stress properties of the work material for machining must be known. The flow stress data obtain from high speed compression tests for a range of plain carbon steels are suitable for making machining predictions⁽¹⁻⁴⁾.

Cutting temperatures are generated in chip formation zone and the tool/chip interface when a metal is machined⁽⁴⁾. Ng *et al*⁽⁵⁾ examined the chips formed under a microscope and observed a secondary deformation zone of approximately 25-50 μ m thickness at the tool/chip interface for a AISI H13 hardened steel. They stated that this zone is an intensively strained zone. Poulachorn and Moison⁽⁶⁾ experimentally investigated the chip formation and chip geometry in hard turning. They showed that the catastrophic shear bands (white bands) can be observed in secondary deformation zone, when machining the AISI E52100 steel at high cutting speeds. It has been reported that in catastrophic shear bands, the temperatures and strain rates are very high^(6,7). Some researchers have said that a white band in tool/chip interface is due to the lack of cooling time to dissipate the heat generated by plastic deformation⁽⁶⁾. Qi *et al* [8] reported that the formation of flow-layer at secondary deformation zone is the result of shear strain. They suggest that the shear strain rate of chip deformation reaches a maximum in this zone. Oxley and his co-workers^(1,2) used a predictive method to determine the thickness of the secondary deformation zone at the tool/chip interface.

Oxley⁽¹⁻²⁾ suggested that the constitutive equation can be obtained from the stress-strain curve of a material for a given strain rate and temperature [$\sigma_1=f(\varepsilon, T)$, $n=f(\varepsilon, T)$],

from compression test results and then expressing these as functions of velocity modified temperature T_{mod} ⁽¹⁻³⁾ thereby obtaining a continuous function of the flow stress properties.

Oxley^(1,2) and Jaspers⁽⁹⁾ showed that the secondary (intense) plastic zone thickness decreased with higher cutting speeds and lower feed rates.

This paper examines with the intense plastic zone thickness (δh_2) at the tool/chip interface for non-heat treated 4140 material and heat-treated 4140 material as well as using the Oxley Machining Theory to predict the cutting forces, chip thicknesses and secondary deformation zones for both materials. A comparison of the results and discussions is presented.

2. The Oxley Theory for Prediction^(1,4)

The development of the theory is discussed in detail in the book by Oxley⁽¹⁾. The basis of the theory is to consider the simple process of orthogonal machining in which the cutting edge is set normal to the cutting velocity.

Fig. 1 shows the model of chip formation for the orthogonal analysis. The model assumes that plane strain, steady-state conditions apply.

$$\begin{aligned}
 F_c &= R_{\cos}(\beta - \gamma) \\
 F_t &= R_{\sin}(\beta - \gamma) \\
 F &= R_{\sin}\beta \\
 N &= R \frac{F_s}{\cos\theta} = \frac{k_{AB}h_1w}{\sin\phi\cos(\phi + \beta - \gamma)} \\
 h_2 &= \frac{h_1 \cos(\phi - \gamma)}{\sin\phi} \\
 V &= \frac{U_{\sin}\phi}{\cos(\phi - \gamma)} \\
 V_s &= \frac{U_{\cos}\gamma}{\cos(\phi - \gamma)}
 \end{aligned} \tag{1}$$

Equation (1) is the geometric relations between the forces in orthogonal machining. Where, it is necessary to determine the shear angle ϕ and the resultant force R . γ is the tool rake angle, β is the mean angle of friction used to describe the frictional condition at tool-chip interface, θ is the angle between the resultant force vector, R , and the shear force vector F_s (fig. 1), k_{AB} is shear flow stress along shear plane AB.

The resultant force R (Fig. 1) transmitted across AB is

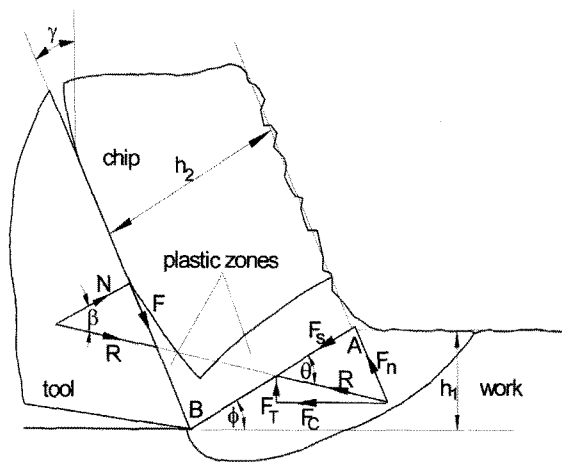


Fig. 1 Orthogonal model of chip formation⁽⁴⁾

calculated for a range of values of ϕ by analysing the stresses along AB. Here, R must be known it is resolved along the tool-chip interface to give the frictional force F.

Oxley reported that by dividing F by the interface area the average value of the interface shear stress τ_{int} is determined (equation 5). For the same range of values of ϕ the temperatures and strain-rates in the boundary layer are calculated and used to determine the average value of shear flow stress in the chip along the interface, k_{chip} (The influence of strain above a strain of $\epsilon=1$ is assumed to have negligible effect on flow stress). The solution for ϕ is taken as the value, which makes $\tau_{int} = k_{chip}$ as the assumed model of chip formation is then in equilibrium.

Once the equilibrium state $\tau_{int} = k_{chip}$ is determined and the shear angle ϕ is known, it is now possible to obtain the chip thickness h_2 and the forces generated during the operation (equation 1). These values are determined using the geometrical analysis of the chip formation zone and the work material properties.

By starting at the free surface just ahead of A and applying the appropriate stress equilibrium equation along AB it can be shown that for $0 < \phi \leq 45^\circ$ the angle θ made by the resultant force R with AB is given by

$$\tan \theta = 1 + 2 \left(\frac{\pi}{4} - \phi \right) - C_n \quad (2)$$

where, C is the constant in the empirical strain rate relation⁽¹⁾ and n is the strain-hardening index in the empirical stress-strain relation. Oxley show that the angle θ

can be expressed in terms of shear angle ϕ , the mean friction angle, β , and the rake angle, γ , by the relation

$$\theta = \phi + \beta - \gamma \quad (3)$$

$$\sigma = \sigma_1 \epsilon^n \quad (4)$$

where, σ and ϵ are the uniaxial flow stress and strain and σ_1 and n is constant which define the stress-strain curve for given values of strain rate and temperature. This is discussed in reference^(1,2).

To determine k_{AB} and n , the average temperature at AB is needed. The average temperature along AB is taken as

$$T_{AB} = T_w + \eta \Delta T_{SZ} \quad (5)$$

where, T_w is the initial work temperature ($= 20^\circ\text{C}$), η ($0 < \eta \leq 1$) is a factor and ΔT_{SZ} is given by

$$T_{SZ} = \frac{1 - \lambda}{\rho S h_1 w} \frac{F_s \cos \gamma}{\cos(\phi - \gamma)} \quad (6)$$

where, ρ is work material density, S is specific heat and λ is the proportion of heat conducted into the work. The proportion of heat conducted λ is developed by Boothroyd⁽¹⁰⁾.

If the intense deformation zone thickness in the tool-chip interface is taken as δh_2 where δ is the ratio of this thickness to the chip thickness h_2 , then the average maximum shear strain at tool-chip interface is found from the equation

$$\dot{\epsilon}_{int} = \frac{V}{\delta h_2} \quad (7)$$

where, V is the rigid chip velocity.

The method used is to calculate for different values of shear angle ϕ the resolved shear stress at tool-chip interface from the resultant force R obtained from the stresses on AB, this is given by

$$\tau_{int} = F / l_c w \quad (8)$$

Oxley and his co-workers in a very early application of the theory for plain carbon steels made that C and δ remain

constant over a range of cutting conditions and have been taken on the basis of experimental results as 5.9 and 0.05 respectively.

The corresponding average temperature at the tool-chip interface is given by

$$T_{int} = T_w + T_{SZ} + \psi T_M \tag{9}$$

where, T_M is the maximum temperature rise in the chip and ψ is factor ($0 < \psi \leq 1$) allows for T_{int} to be an average value. Boothroyd [10] calculated T_M using a numerical method by assuming a rectangular plastic zone (heat source) at the tool-chip interface.

To be useful in predictive cutting performances, the material properties, such as flow stress, strain, chemical composition and thermal properties, must be obtained. Hastings and Oxley⁽¹⁾ used with the flow stress by Oyane *et al*⁽¹¹⁾ from high-speed compression tests. Oyane [11] tested plain carbon steels with carbon contents ranging from 0.16~0.55%. Although their strain rates ($\approx 450/s$) was lower than generally encountered in machining ($10^3\sim 10^6/s$), the testing temperatures covered a wide range (0~1100 °C). The compression test results of Oyane *et al*⁽¹¹⁾ allowed the extrapolation of the results into the machining range by using the Velocity Modified Temperature concept suggested by McGregor & Fisher⁽¹²⁾. This can be written as

$$T_{mod} = T(1 - v/g\varepsilon/\varepsilon_0) \tag{10}$$

where, T is cutting temperature, the strain rate with v and are constants which are taken as 0.09 and $1s^{-1}$.

3. Experimental Work

3.1 Material properties for Work Materials

The material properties are a determining factor in obtaining the work material cutting performance. Medium carbon alloy steel AISI 4140 can be machined in a turning operation without coolants. The chemical compositions of

Table 1 Chemical composition of AISI4140 steel (% weight)^(4,13)

| C | P | Mn | Si | Ni | Cr | Mo | Cu |
|------|-------|------|------|------|------|------|------|
| 0.44 | 0.016 | 0.94 | 0.23 | 0.09 | 1.13 | 0.19 | 0.21 |

these materials are shown below in Table 1.

The author used a Vickers hardness tester (Model: AVERY 6406) to measure the hardness values, and then the author converted results to Rockwell hardness values. The hardness of the two bars are shown in Table .2.

The density, thermal conductivity and specific heat of the material are presented in Table .3, where, T is cutting temperature.

Lacking information on the flow stress properties of AISI 4140 material, it was decided to use the flow stress curves for the 0.44% plain carbon steel, since this information is available for the Oxley machining theory⁽¹³⁾. Earlier work has indicated that the carbon content has significant effect on the work material properties.

Fig. 2 shows the 0.44% plain carbon steel flow stress curves for the virgin and heat treated material. As shown figure 2, σ_1 decreases with increase in temperature. It should be noted that the heat-treated material has a hardness value of 45HRC which is approximately 40% above that of the

Table 2 Hardness of AISI 4140^(4,13)

| Non-heat-treatment | Heat-treatment |
|--------------------|----------------|
| 27HRc | 45HRc |

Table 3 Temperature dependent thermal properties used as inputs to the cutting theory⁽¹³⁾

| | |
|-------------------------------|---|
| Density | 0.00758 g/mm ³ |
| Thermal conductivity (K) | 49.84-0.0242T (W/m°C) |
| Specific heat (ρc), S | 3124025.8 + 6480.2T - 4.3235T ² (J/m ³ °C). |

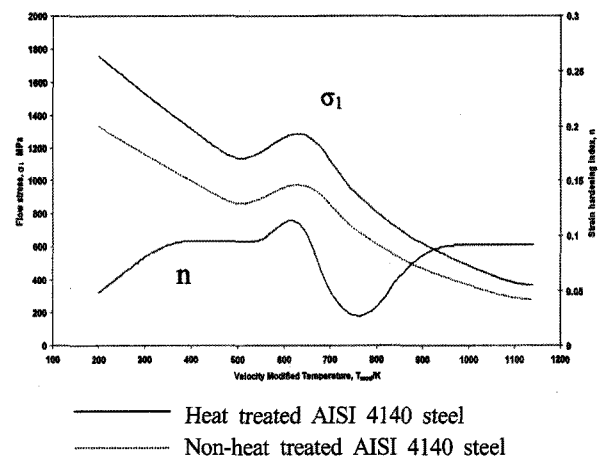


Fig. 2 Flow stress properties of work material^(4,13)

virgin material. The work carried out by authors⁽¹⁴⁾, it was reported that the increase in hardness is related directly to the strength of the material. Therefore, the author had assumed an increase of 40% in the value of σ_1 across the velocity modified temperature range.

However, the strain hardening index was not changed n . In the early work by Oxley and his co-workers^(1,2), it was found that the carbon content influenced the flow stress more than the strain-hardening index, n .

To make all of the necessary calculations in the present work, C-computer program was used. The input data to the program includes: work material chemical composition, tool geometry, cutting condition and etc.

3.2 Cutting Conditions

The heat-treated bar is 110mm in diameter and 200mm length while the virgin material is nominally 110mm in diameter and 300mm in length. The cutting condition is shown below in Table 4.

3.3 Experimental Set up and Procedure

The cutting tests were carried out using the following table 4.

Cutting forces are collected in the z direction (F_z), x direction (F_x) and y direction (F_y) using a Kistler piezoelectric 3-axis dynamometer. After machining, the average chip thickness (h_2) is obtained by using the length of chip and weight of chip as it is assumed that the density and width of chip are constant during the process.

To investigate the experimental values of secondary plastic

zone thickness to the chip thickness samples of chips are mounted, polished and etched using standard metallurgical techniques.

The simple case of orthogonal machining where the tool has zero inclination is carried out for this investigation where the approach angle is not zero but 45° .

It is known that the magnitude of y -component is dependent on nose radius of cutting tool. In these experiments the radius will be assumed to be equal to zero though it has a value of 0.4mm. Therefore, radial force (F_r) can be neglected when determining the cutting (F_c) and thrust force (F_T). Accordingly, thrust force is determined by following as equation (11):

$$F_c = F_z \tag{11}$$

$$F_T = F_x \cos C_s + F_y \sin C_s$$

In Orthogonal machining condition where side cutting edge angle is not zero, the values of uncut chip thickness (h_1) and the width of cut (w) are determined as follow (assuming zero nose radius) equation (12):

$$h_1 = f \cos C_s \quad w = d / \cos C_s \tag{12}$$

4. The Predicted and Experimental Results

Fig. 3 shows the comparison of the predicted and experimental cutting and thrust force results for both virgin and heat treated steels. The predicted results are shown with lines while the experimental results are shown with symbols. A direct observation shows that the predicted results for the heat treated steel is higher than those of the virgin material for the cutting force component (Fig. 3a). This is in agreement with the experimental results. Again the trend is observed where the forces decrease with increase in cutting speed.

However it is observed that the experimental cutting forces for the virgin material is slightly higher than those of the hardened material at speeds above 200m/min for the feeds of 0.1 and 0.14 mm/rev. At the feed of 0.05mm/rev the predicted value of cutting force is low compared to the experimental result. This is probably due to formation of built-up edge at this speed for the virgin material therefore an incorrect prediction can occur⁽¹³⁾.

Table 4 Experimental Set up

| | | |
|-------------------|---------------|---|
| Cutting Tool | Insert | SNGA 120404T |
| | Tool Holder | PSDNN 2525M-12 |
| | Tool Geometry | -7° Rake angle(γ) 45° Approach angle (Cs) |
| Cutting Condition | Cutting Speed | 50,100,200,300,400m/min |
| | Feed Rate | 0.05, 0.1,0.14mm/rev |
| | Depth of cut | 0.5mm |
| Test Equipment | | Heindenreich and Harbeck lathe |
| Machining process | | Orthogonal cutting tests |
| Data collection | | Kistler piezoelectric 3-axis dynamometer |

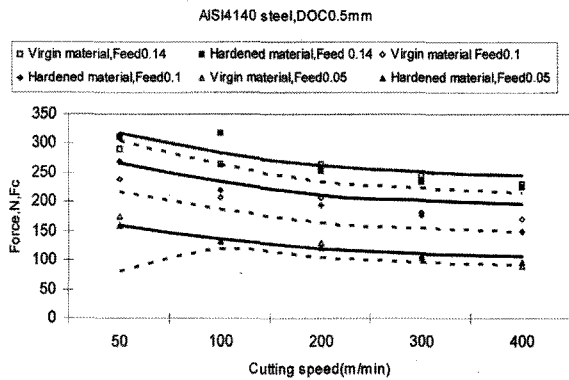
Fig. 3b shows the results for the thrust force and it can be seen that similar trends as for the cutting forces are observed. However it is interesting to note that the thrust force for the virgin material is higher than that for the hardened material at a feed of 0.14mm/rev and the same result is observed for the experimental results. The opposite trend is observed for the lower feed rates with the hardened material results being higher than the virgin material results as seen in the experimental results. The possible reason for the higher thrust force for the feed rate of 0.14mm/rev is that the shear angle is larger for the virgin material and thus resulting in a higher thrust force. This was mentioned earlier ⁽¹⁾.

Fig. 4 shows the results for the chip thicknesses obtained. The predicted results show that the chip thickness for the virgin material is higher than those for the hardened material. In addition as the speed increases the chip thickness decreases. This is indicated by the experimental

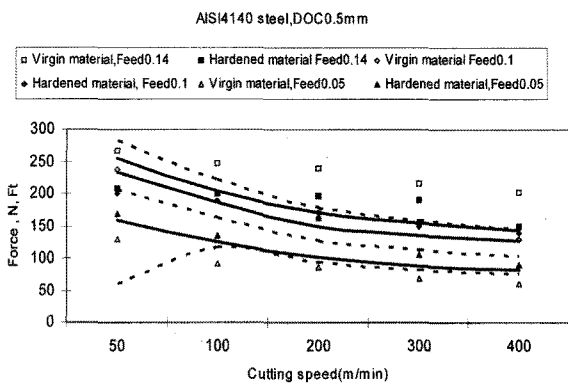
results as well. However it can be seen that the experimental results are lower than the predicted results. The reason for this is that there could be side spreading of the material at the depths of cut that have used and this will result in a thinner chip as well as the result of measurement errors ^(13,15). It is important to note that the trends predicted and experimentally observed are similar.

Fig. 5 shows the predicted and experimental results for the secondary deformation zone for both the virgin and heat treated materials. It can be seen that the predicted results show a decreasing trend as the speed increases for both materials. A decreasing trend is observed for the virgin material with the experimental results being lower than the predicted results. In the case of the heat-treated material, the experimental results show a constant trend across the cutting speeds. This could be the result of the material hardness obtained after heat treatment. The heat treatment has changed the material flow stress characteristics thus resulting in a white layer for the secondary deformation which is affected by the strain-rate and temperature attained in the secondary deformation zone. The predicted results show a decreasing trend as the speed increases. This is the result of using the flow stress properties for plain carbon steel. In this work the effect of crystalline structure has not been taken into account and the results obtained are purely the result of continuum mechanics. However it is important to note that the order of magnitude for the secondary deformation zone size is the same for both the predicted and experimental results.

These results show that the Oxley Machining Theory can be used to predict the forces in hard turning as long as the work material properties are known.



(a) Cutting Force, F_c



(b) Thrust Force, F_T

Fig. 3 Predicted and experimental cutting forces for the virgin and heat treated 4140 steel; Solid line is predictive heat treated material and Dot line is predictive virgin material, all symbols are experimental data

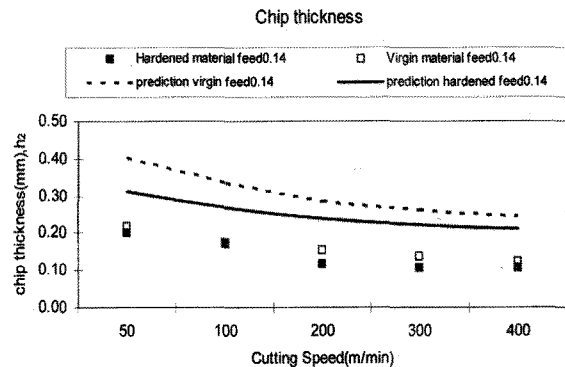


Fig. 4 Predicted and experimental chip thickness for AISI 4140 steel

The results in Fig. 6 show the photomicrographs classifying the secondary deformation zone for different cutting speeds⁽¹³⁾. It can be observed from these figures that the flow lines from the chip deform greatly at the tool/chip interface as the cutting speed increases and also the size of the secondary deformation zone changes as the speed changes. Fig. 6 (a) indicates that the secondary deformation zone is difficult to observe for the low cutting speeds but easy to see at the high cutting speeds due to the formation of a white layer at the tool/chip interface. Therefore the deformation zone for the low cutting speeds is assumed to occur where a change in the slope of the flow lines is observed near the tool/chip interface. This is indicated by the lines drawn on the photomicrographs.

In the case of the hardened material the secondary deformation zone at tool/chip interface can be clearly observed at low cutting speed due to the formation of the white layer. It is also noted that as the cutting speed increases the secondary deformation zone increases slightly in size.

It can also be observed that the chip formation changes from a continuous chip to a saw tooth chip at the speed increases. The saw tooth formation is definitely pronounced in the hardened material. In addition there is a zone of intense deformation between the peaks of the saw tooth formation in the hardened material. Though there is saw tooth formation at the high speed for the virgin material there is no intense deformation zone between the peaks.

5. Conclusions

The discussions above lead to the following conclusions:

- (1) Although the hardness of heat-treated 4140 steel is approximately 40% higher than non heat-treated 4140 steel, the heat treated material is the resulting forces only vary by 10%. This reason for this varies could be that the temperature at the interface increases due to the harder work material (Increased strength)⁽¹³⁾.
- (2) The chip thickness of heat treated 4140 steel is lower than those of non-heat treated 4140 steel. This possible reason that the reduction of chip thickness with the increase of work material hardness results from increasing the shear angles
- (3) There is a significant white layer for the secondary deformation zone when machining the hardened work

material and the white layer can be observed in the virgin material at high cutting speeds. In the case of the heat treated material, the experimental results show a constant trend across the cutting speeds. This could be the result of the material hardness obtained after heat treatment. The heat treatment has changed the material flow stress characteristics thus resulting in a white layer for the secondary deformation which is affected by the strain-rate and temperature attained in the secondary deformation zone. The predicted results show a decreasing trend as the speed increases. This is the result of using the flow stress properties for plain carbon steel. In this work the effect of crystalline structure has not been taken into account and the results obtained are purely the result of continuum mechanics⁽¹⁵⁾.

- (4) The Oxley Machining Theory can be used to predict the cutting performance factors for hard turning as long as the correct work material properties are used. In this paper the plain carbon steel flow stress properties were used.

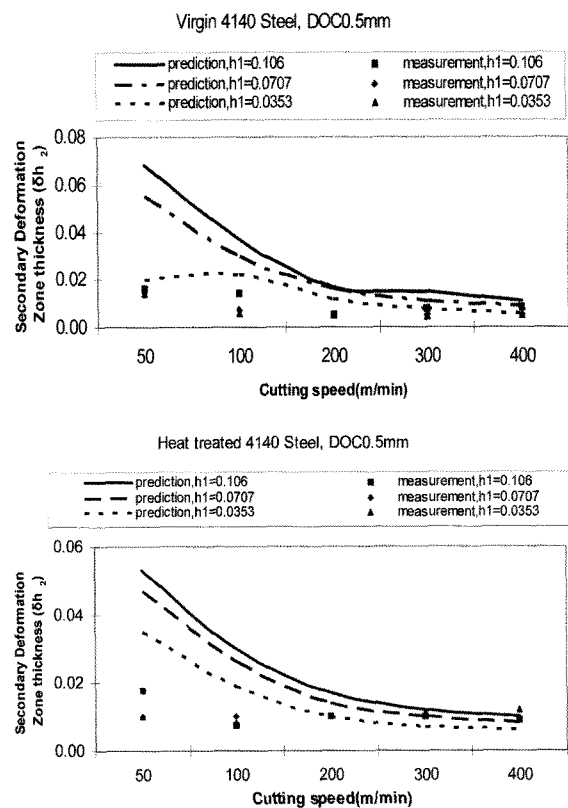


Fig. 5 Predicted and experimental tool/chip interface plastic zone thicknesses: where the lines are the predicted values using Oxley theory

References

- (1) Oxley, P. L. B., 1989, *Mechanics of Machining: An Analytical Approach to Assessing Machinability*, Halsted Press, New York.
- (2) Mathew, P., and Oxley, P. L. B., 1981, "Allowing for the Influence of Strain Hardening in Determining the Frictional Conditions at the Tool/Chip Interface in Machining," *Wear*, Vol. 69, Issue 2, pp. 219~234.
- (3) Kopac, J., Korosec, M., and Kuzman, K., 2001, "Determination of Flow Stress Properties of Machinable Materials with Help of Simple Compression and Orthogonal Machining Test," *Int. J. Mach. Tool Manuf.*, Vol. 41, Issue 9, pp. 1275~1282.
- (4) Becze, C. E., Worswick, M. J., and Elbestawi, M. A., 2001, "High Strain Rate Shear Evaluation and Characterization of AISI D2 Tool Steel in Its Hardened State," *Mach. Sci. and Tech.*, Vol. 5, Issue 1, pp. 131~149.
- (5) Ng, E. G., and Aspinwall, D. K., 1999, "Modelling of Temperature and Forces when Orthogonally Machining Hardened Steel," *Int. J. Mach. Tool Manuf.*, Vol. 39, Issue 6, pp. 885~903.
- (6) Poulachon, G., and Alphonse L. M., 2000, "Hard Turning: Chip Formation Mechanisms and Metallurgical Aspects," *Tran. of the ASME*, Vol. 122, pp.406~412.
- (7) Becze, C. E., and Elbestawi, M. A., 2002, "A Chip Formation Based Analytic Force Model for Oblique Cutting," *Int. J. Mach. Tool Manuf.*, Vol. 42, Issue 4, pp. 529~538.
- (8) Qi, H. S., and Mills, B., 2003, "Modelling of The Dynamic Tool-chip Interface in Metal Cutting," *J. of Material Pro. Tech.*, Vol. 138, Issues 1-3, pp. 201~207.
- (9) Jaspers, S. P. F. C., and Dautzenberg, J. H., 2002, "Material Behaviour in Metal Cutting: Strains Strain Rates and Temperature in Chip Formation," *J. of Material Pro. Tech.*, Vol. 121, Issue 1, pp. 123~135.
- (10) Boothroyd, G., 1963, "Temperatures in Orthogonal Metal Cutting," *Proc. Instn mech. Engrs*, Vol. 177, pp. 789~802.
- (11) Oyane, M., and Takashima, F., 1967, The Behaviour of Some Steels Under Dynamic Compression, *10th Japan congress on testing materials*, pp.72.
- (12) McGregor, C. W., and Fisher, J. C., 1946, "A Velocity Modified Temperature for the Plastic Flow of Metals," *J. Appl. Mech.*, Vol. 13, A11~A16.
- (13) Lee, T. H., and Mathew, P., 2005, "An Experimental and Theoretical Comparison of Machining Non-heat Treated and Heat Treated AISI 4140 Steel," *8th CIRP International Workshop on modeling of machining operations*, Chemnitz, Germany, pp. 293~302.
- (14) Stephenson, D. A., and Agapiou, J. S., 1997, *Metal Cutting Theory and Practice*, Marcel Dekker Inc.
- (15) Lee, T. H., 2007, *An Experimental and Theoretical Investigation for The Machining of Hardened Alloy Steels*, A Thesis for a Doctorate, School of Mechanical and Manufacturing Engineering, the University of New South Wales, NSW, Australia.